IPPI

Polyolefins Journal, Vol. 8, No. 2 (2021)
DOI: 10.22063/poj.2021.2823.1172

ORIGINAL PAPER

Kinetic study on liquid propylene polymerization using a modified heat flow reaction calorimeter

Mehrsa Emami*, Farzin Hormozi, Hossein Abedini

Department of Process and Modeling, Iran Polymer and Petrochemical Institute, P.O. Box 14185/458, Tehran, Iran

Received: 23 December 2020, Accepted: 5 June 2021

ABSTRACT

Bulk phase polymerization of propylene with a 4th generation of Ziegler-Natta catalyst was kinetically investigated by means of heat flow calorimetry. The assumptions and modifications on isothermal calorimetric method were demonstrated. Our calibration method showed that heat exchange with the reactor cover plate is not constant over time. Therefore, the dynamic of cover plate temperature was considered in the calorimetric method. The polymerization rate profiles depending on hydrogen and external electron donor concentration have been investigated. Normalized polymerization profiles (R_p/R_{pmax}) are plotted and expressed as an exponential function of time. Effects of hydrogen and external electron donor (ED) concentration on R_{pmax} and polymerization rate were investigated as well. The results showed that by increasing hydrogen concentration, initial polymerization rate (R_{pmax}) increased. Hydrogen increased productivity by increasing the initial polymerization rate, while it had no negative effect on the rates of decay or its effect was small. The ED concentration was optimized so that the catalyst deactivation rate was at its lowest level. Also, changes in the ratio of activation to inactivation with ED concentration were examined, and a proportional change was observed. **Polyolefins J (2021) 8: 123-133**

Keywords: Kinetic study; calorimetry; liquid monomer; propylene; polymerization.

INTRODUCTION

In heterogeneous propylene polymerization, particle morphology and polymer molecular properties are extremely relevant to the kinetic of the reaction. Generally, the polymerization rate can be determined experimentally by measuring the change in any property (such as solubility, refractive index and density) or reactor conditions (temperature, pressure and flows) during the course of the polymerization [1]. Flow rate technique, dilatometry and calorimetric approach are different utilized techniques to estimate the polymerization rate [2,3]. Flow rate technique is based on monomer consumption which can be easily calculated by the amount of monomer fed into the reactor, since gross reaction rate of the polymerization reaction in semi-batch experiments (at isothermal conditions) is proportional to the monomer consumption [4-5]. The

---

*Corresponding Author - E-mail: m.emami@ippi.ac.ir

first article reporting rate profiles in catalytic liquid propylene polymerization using calorimetric measurements was published by Samson et al. [6].

In dilatometry technique, volume changes caused by chemical reaction are measured and correlated to the reaction kinetics. Reaction calorimetry is a powerful technique to determine conversion by estimation of the heat generated by the reaction, which has been known since 1982 [7].

Although reaction calorimetry was widely used for free radical polymerization processes, it had not found application in catalytic olefin polymerization until 1998s [6, 8]. Most olefin polymerization techniques are conducted in the semi-batch. In these conditions, flow meter technique is the first choice to study the polymerization rate via monomer gas consumption measurement. In the isothermal bulk phase propylene polymerization, the overall reactor pressure is constant and correlates with the vapor pressure of the liquid monomer. Consequently, the approach described for flow rate technique is not applicable. Dilatometry is limited by difficulties in sampling methods at high pressure and only leads to discontinuous conversion-time curves [1]. To overcome these drawbacks, Samson et al. utilized reaction calorimetry and published an article using calorimetric method rate profiles in catalytic liquid propylene polymerization in 1998 [6].

Afterwards, various calorimeters have been designed and developed in the literature to study propylene polymerization reactions [10-12]. Moderate improvements in calorimetric methods to study the kinetics of bulk phase propylene polymerization have been published by Samson 1999, Shimizu 2001 and Pater et al. 2002 [13-15].

Evolution of the overall heat transfer coefficient during the reaction limits calorimetric techniques. Mckenna et al. developed a calorimetric method that did not require the data of the overall heat transfer coefficient changes, as well as the heat loss term [16].

Korber et al. 2001 used heat flow calorimetry for the investigation of the slurry-phase polymerization of propylene. They concluded that in the range of low activity reactions, other techniques except for calorimetry were not able to deliver precise information about the polymerization kinetics. They assumed a constant value of UA remained during the experiments [17].

A reaction calorimeter to follow slurry-phase polymerizations of ethylene with supported catalysts has been introduced by Tisse et al. They assumed negligible heat loss and used an approach using a high gain observer to evaluate the initial value of UA (the product of the overall heat transfer coefficient and the heat transfer surface area). They also demonstrated that in the solid content less than 30%, estimation of UA during the reaction was not necessary [5].

Kettner et al. presented a calibration-free and a developed method for online baseline correction in a heat flow calorimeter. They applied those methods for kinetic studies of propylene bulk phase polymerization [11].

Theory of calorimetry consists of only two laws: the law of heat transfer and the law of conservation of energy. The reaction mass is considered to be perfectly mixed, and changes in kinetics, potential energies and heats of mixing and solution are neglected [12].

Depending on how the reaction temperature is controlled, reaction calorimeters are classified as follows:

(i) Isothermal: the reactor temperature is controlled at a constant level.

(ii) Adiabatic: the jacket temperature is controlled to avoid heat losses.

(iii) Isoperibolic: the jacket temperature is controlled at a constant level, so the reactor temperature is not controlled [18, 19].

In this article, moderate heat flow calorimetry was introduced to investigate the bulk phase polymerization of propylene with Mg/Cl_2-supported Z-N catalyst. Assumptions and modifications on the isothermal calorimetric method were demonstrated. Effect of reactor cover temperature variations on the system heat dynamic was not neglected. This considered due to its mass and led to the minimization of errors. Normalized polymerization profiles (R_p/R_{pmax}) were plotted and expressed as an exponential function of time. Effect of hydrogen and external electron donor on R_p/R_{pmax} profile and the exponential function parameters were discussed.

THEORY AND MODELING

Generally, calorimetric measurement is based on a simple dynamic model and a macroscopic kinetic relationship between the heat released from the reaction and the rate of monomer consumption. The basis of a calorimetric measurement is the heat balance of a stirred-tank reactor. The energy balance around a stirred tank reactor is:

$$Q_{acc} = Q_r + Q_{jacket} - Q_{loss} \tag{1}$$

Equation 1 must be solved to estimate Q_r which is heat generated by the exothermic chemical reaction. Other expressions in Equation 1 must be directly measured or estimated [20]. Heat-flow rate during a chemical reaction is proportional to the reaction rate, this can be expressed in terms of the following mathematical expression:

The rate of reaction, R_p, can be calculated from Equation 2 by estimating the heat released from the reaction, Q_r (J s^{-1}):

$$Q_r = R_p H_r m_{cat} \tag{2}$$

Calorimetry implementation steps

Experimental Setup

The experimental setup for liquid pool polymerizations includes a 4-L stainless steel jacketed reactor and feeding systems to measure propylene and hydrogen. The heating-cooling system, including cold water and super heat steam pipes, pneumatic valves and a proportional-integral (PI) control unit, is illustrated in Figure 1. ICPCON modules were implemented as data acquisition system to monitor and save the reactor and the inlet and outlet jacket temperatures.

Calorimetry steps

Figure 2 represents the flowchart of our calorimetric implementation steps which includes:

- √ Process dynamic behavior modeling using a simple model
- √ Comparing model predictions with experimental data in the absence of exothermic chemical reaction. The reactor is filled only with the reaction medium (liquid propylene).
- √ Compensation for model deviation from experimental data
- √ Determination of heat generation estimation algorithm based on the modified model
- √ Preliminary calibration
- √ Analyzing the performance of estimators in stable and dynamic states

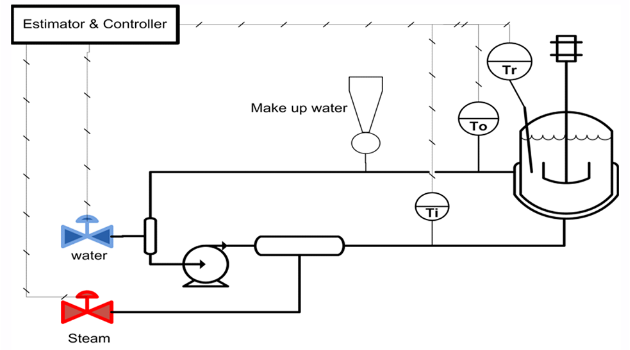

Figure 1. Experimental setup including heating-cooling system consisting of cold water and super heat steam pipes, pneumatic valves and a proportional-integral (PI) control unit.

Process dynamic behavior modeling using a simple model

Dynamic Model

A simple model was used to describe the dynamic

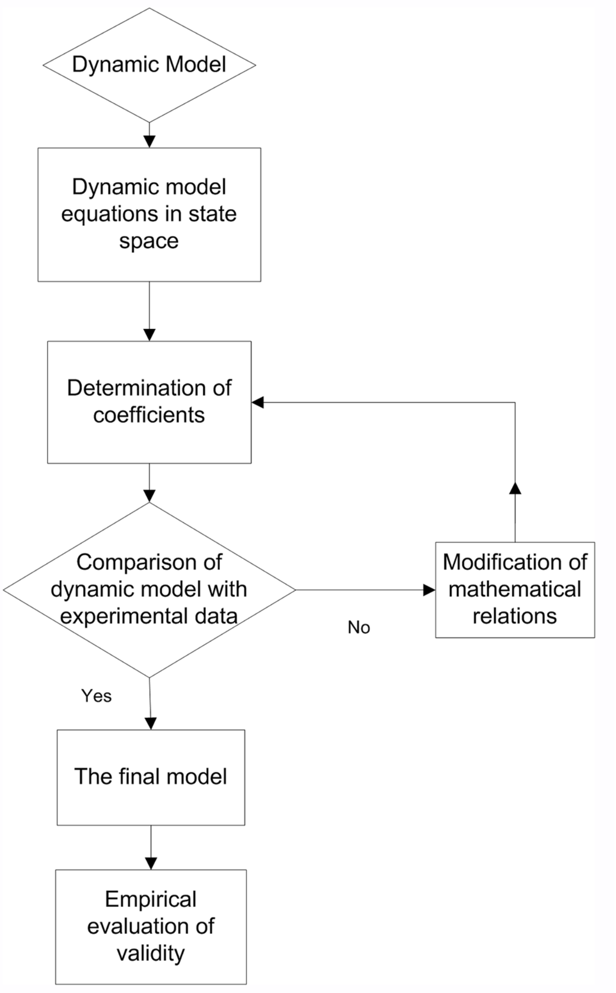

Figure 2. Flowchart of calorimetry steps.

temperature of the reactor, assuming the existence of an overall heat transfer coefficient:

Heat balance of the reactor can be expressed as equations 3:

$$\frac{dT}{dt}=\frac{(Q_r-Q_b)+u_i.A_i.(T_j-T)}{m.C_p} \tag{3}$$

Heat balance of the reactor jacket can be expressed as:

$$\frac{dT_j}{dt}=[u_i.A_i(T-T_j)+U_\infty.A_\infty(T_\infty-T_j)+\frac{F_w.\rho_w.C_w}{1-\gamma}.(T_{ji}-T_j)]/(m_j.C_w) \tag{4}$$

Jacket temperature was assumed as a linear average of inlet and outlet jacket temperatures:

$$T_j=T_{jO}-\gamma.(T_{jO}-T_{ji}) \tag{5}$$

Considering the time constant of the sensors, we will have:

$$\frac{dT_m}{dt}=\frac{1}{\tau_m}(T-T_m) \tag{6}$$

$$\frac{dT_{j,m}}{dt}=\frac{1}{\tau'_m}(T_j-T_{j,m}) \tag{7}$$

The term Q_b represents the interaction of the system with the environment, and all other additional heat inputs and outputs, like stirrer dissipation, heat exchange with the cover plate, and so on. This term was assumed constant over time, as it is considered constant by Samson and other authors [13-15].

Assumptions used were:

1- The heat generated by the stirrer is taken into account in the numerical value of Q_b
2- The dynamic effect of the reactor wall between the reactor contents and the fluid inside the jacket is considered in the overall heat transfer coefficient
3- Linear correlation of jacket temperature with inlet and outlet jacket temperatures (T_{ji}, T_{jo})
4- F_w (flowrate of cooling water into the jacket) was assumed to be fixed
5- Q_b was assumed constant over time

Mathematical analysis in state space

The goal is to develop our model in the form of state equations. By separating the variables and model constants, the variables have been divided into four groups. These were state space variables, load variables, control variables and measurement variables.

State space variables:

In our model, reactor and jacket temperatures were determined by differential equations in the model. These terms were space state variables and defined as:

$$x_1=T_j, x_2=T \qquad X^T=[x_1\ ,\ x_2] \tag{8}$$

Load variable: Are a set of external factors that can take the system temperature out of the set point. With this assumption, the load variable can be considered as the sum of the two variables of reaction heat value Q_r and balance variable Q_b. We express these variables in the form of a variable (L) as:

$$L=\frac{Q_r-Q_b}{m.C_p} \tag{9}$$

The term Q_b was assumed constant over time, as mentioned earlier.

At the steady state conditions, the load variable can be proportional to the temperature difference between the reactor temperature (T_r) and the jacket temperature (T_j).

Control variable: Inlet jacket temperature T_{ji} was defined as control variable. Term U can be defined as a function of T_{ji} as:

$$U=\frac{u_\infty.A_\infty}{m_j.C_w}.T_\infty+\frac{F_w.\rho_w.C_w}{m_j.C_w(1-\gamma)}.T_{ji} \tag{10}$$

All terms in the equation 10 are constant.

Two terms L and U, which are external actions, were determined by equations 9 and 10.

In equations 9 and 10, variable L is not predictable and variable U must be adjusted by the controller.

Measurement variables: The outputs of the temperature sensors are state variables that can be considered as state variables. Measurement variables can be predicted by mathematical model. Measuring variables was defined as:

$$y_1=T_m\ ,\ y_2=T_{j,m}\ ,\ Y^T=[y_1\ ,\ y_2] \tag{11}$$

Using these definitions, the mathematical model can be rewritten in the form of state equations.

Using these definitions, the model (equations 3 and 4) can be rewritten in the form of state equations:

$$\begin{aligned} X_{(k)} &= A.X_{(k-1)} + B.\varphi_{(k)} \\ Y_{(k)} &= C.Y_{(k-1)} + D.X_{(k)} \end{aligned} \tag{12}$$

In these equations, *A, B, C* and *D* are the constant coefficients, *X* is the state variable matrix, *Y* is the measurement variable matrix and matrix φ is defined as:

$$\varphi^T = [L\,, U] \tag{13}$$

Matrixes *A, B, C, D* are defined in the appendix.

Determination of constant coefficients

To determine constant coefficients *A, B, C* and *D* in equation 12, the reactor was filled with liquid monomer. Then, the temperature of the reactor increased and decreased several times by changing reactor set point. In each set point, the reactor temperature was kept constant for some time. Reactor temperature changes were plotted and constant coefficients were determined by trial and error (Figure 3). In Figure 3, comparison of our model prediction and experimental data is illustrated. The deviation of model from experimental data in Figure 3 can be relevant to a dynamic phenomenon. This deviation can be attributed to the reactor cap (cover plate), which has a high heat capacity due to its high thickness. The reactor cover plate acted as a hot object when the reactor was heated up and acted as a hot object when the reactor was cooled down. Therefore, we have included the cover plate temperature in the form T_M° in Q_b.

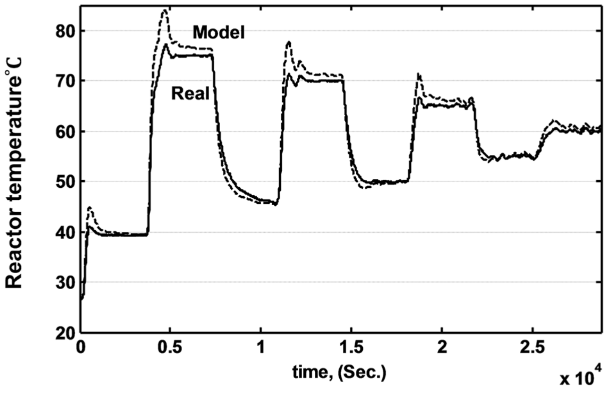

Figure 3. Initial tuning of the model predictions for reactor temperature with experimental data to determine the model coefficients: (---) model prediction (___) experimental data.

Comparing the model with experimental data and modification using compensator equations

As mentioned above, we assumed the mismatch between model and experimental data in Figure 3 is relevant to the reactor cover plate. Considering cover plate temperature (T_M°) in Q_b leads to:

$$\begin{aligned} Q_b &= C_1.T_M^\circ + C_2(\,T_M - T_\infty) \\ T_M^\circ &= \frac{1}{\tau_M}(\,T_r - T_M) \end{aligned} \tag{14}$$

Where, T_M° is the cover plate temperature and τ_M is the time constant of response. C_1 and C_2 are constants which were determined by trial and error.

In Figure 4, a comparison of model prediction and experimental data (considering heat dynamic of the reactor cover, T_M°) is plotted. Figure 4 shows a good agreement of the model prediction with the experimental data.

Heat Release Estimators (Heat Observers)

In the state space, unknown load variable can be related to other known variables, measurement and control variables using the discrete form of equations 12:

$$L_{(K)} = \frac{y_{1,(k)} - y_{1,(k-1)}}{\Delta t} - a_{11}.y_{1,(k)} - a_{12}.y_{2,(k)} \tag{15}$$

Note that in equation 15, the measurement variables are substituted for the state variables, because in prac-

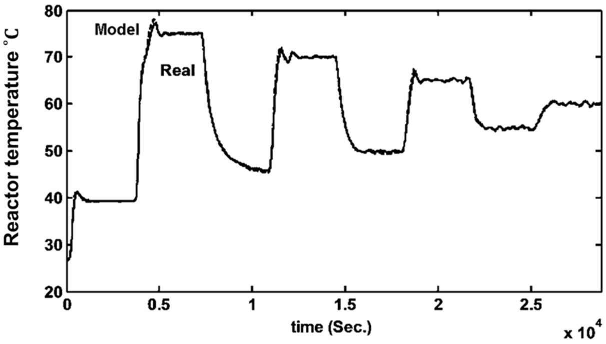

Figure 4. Comparison of modified model prediction at the reactor temperature from actual data: (---) model prediction (___) experimental data.

tice, measurement variables are available.

Applying both reactor and jacket heat dynamics to equation 15 leads to:

$$L_{(k)} = \frac{\beta}{(1+a_{22}.\Delta t).\Delta t}.y_{1(k)} - \frac{1}{\Delta t}.y_{1,(k-1)} - \frac{a_{12}}{(1-a_{22}.\Delta t)}.y_{2,(k-1)} - \frac{a_{12}.\Delta t}{1-a_{22}.\Delta t}.U_{(k)} \qquad (16)$$

Estimator (15) operates only with the temperature signals (y_1 y_2), while estimator (16) operates with the both temperature and controller signals.

The state estimators, introduced by Equations 15 and 16 are the amount of heat released at each point, showing the sampling process. The heat released can be attributed to the reaction rate according to Equation 2.

Calibration

To guarantee the operation of estimators, a calibration method was used. This preliminary calibration is based on the fact that "the heat generation is zero when the reaction does not occur". By making a series of step changes at the set point, the experimental data required for the preliminary calibration were obtained. In this case, the estimator must be adjusted so that the isothermal baseline areas of the heating line conform to zero.

Figure 5 illustrates the result of calibration method. The results showed that although estimations were valid in the steady conditions, dynamic regions could not be predicted.

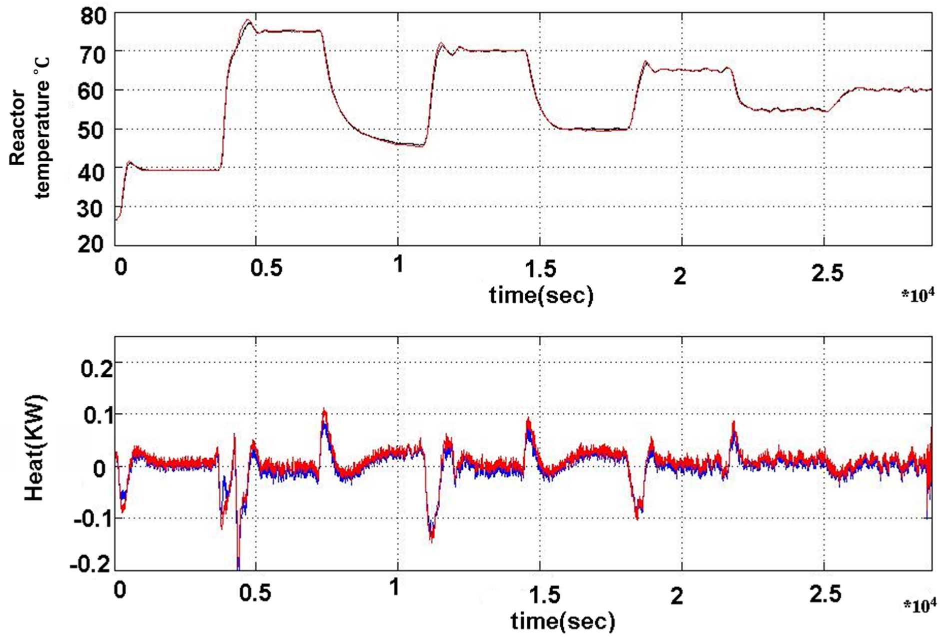

Figure 5. Estimator calibration, assuming zero heat generation in the isothermal regions, Up: (---) Model prediction and (___) experimental data, Down: base line calibration curve.

Kinetics model

Kinetics of olefin polymerizations with Ziegler-Natta catalysts were described with a first-order model. Assumptions used for a 4th generation of catalytic system were:

(a) Polymerization rate is proportional to monomer concentrations and the number of catalyst active centers,

(b) Active center number decreases with the reaction progress exponentially, and

(c) Mass transport limitations in expanding particles is negligible.

Thus, the kinetic model can be written as:

$$R_p = R_{p\max} \exp(-k_d t) \qquad (17)$$

For our experiments at constant pressure, the reaction heat flow rate can be expressed as equation 2.

To calculate the reaction enthalpy, we used the equation:

$$\Delta H_r = \frac{\sum Q_r.\Delta t}{mileage} \qquad (18)$$

The mileage is proportional to R_p:

$$mileage = \sum(R_p.m_{cat}.\Delta t) \tag{19}$$

Data file, including reactor, inlet and outlet jacket temperature over a sampling time (10 s) were achieved experimentally.

The value of the heat released was calculated by equations 14 and 18.

Monomer consumption can be extracted by equation 2 over each sampling time as:

$$R_p = \{R_1, R_2, \ldots, R_n\} \tag{20}$$

It was explained that the results of estimation were not accountable in the dynamic region. So the subset from data that is suitable for kinetic study is:

$$\widetilde{R}_p = \left\{\widetilde{R} \subset R_p \middle| \{R_m, R_{m+1}, \ldots, R_n\}, m = 100, n = 360\right\} \tag{21}$$

Also, it is known that the rate profile of monomer consumption curve is decayed naturally.

$$R_{\max} = \max\{R_{100}, R_{101}, \ldots, R_{360}\} = R_{100} \tag{22}$$

The normalized form of $\widetilde{R}_p$ can be defined as follows:

$$\frac{R_p}{R_{\max}} = \left\{1, \frac{R_{101}}{R_{100}}, \ldots, \frac{R_{360}}{R_{100}}\right\} \tag{23}$$

The set of functions generated by an arbitrary function can be chosen as a macroscopic behavior of monomer consumption.

$$\frac{R_p}{R_{\max}} = 1 + e^{-at} - e^{-bt} \quad , \quad a,b > 0 \tag{24}$$

Where, the term a was considered as activation intensity, and *b* was defined as deactivation intensity. Thus, the ratio *a/b* can be considered as activation to deactivation intensity. For each experiment, coefficients *a* and *b* were found by trial and error.

EXPERIMENTAL

Materials

The catalyst system was a commercially available spherical $MgCl_2$-supported Ziegler-Natta catalyst of 4th generation supplied by Basell Polyolefin’s Co. Triethyl aluminum (TEA of 98% purity) from Maroun Petochemical Co., diluted in n-hexane was used as cocatalyst and the so-called C-donor (cyclohexyl methyl dimethoxy silane) supplied from Basell Polyolefin’s Co., was used as external electron donor. Polymer grade propylene, hydrogen and nitrogen were provided from Maroun Petrochemical's and were used as received.

Polymerization procedure

To start a polymerization experiment, the reactor was first cleaned at 80°C. A flow of hot nitrogen was passed through the reactor and connected lines, at least for 8 h, to remove all impurities from it. Prescribed amount of catalyst, cocatalyst (TEAl), and external electron donor (C-donor) were separately transferred to the catalyst injection system. Activated catalyst was injected into the reactor. Then, the reactor was filled with a prescribed amount of hydrogen and 2.6 L of fresh, liquid propylene for polymerization. Then reactor temperature was raised to polymerization temperature (70°C). A non-isothermal pre-polymerization, proposed by Pater et al. [14] was used. After the prescribed polymerization time, the reaction was stopped by cooling and opening the vent valve, simultaneously, allowing the unreacted monomer to evaporate quickly.

RESULTS AND DISCUSSION

Reproducibility

First of all, reproducibility of the experiments was proved. This was tested by repeating a standard experiment for three times. Experiments were run at different amounts of the catalyst with 0.05 mol of hydrogen, at 70°C and 37 bar. The external donor to cocatalyst ratio was fixed at these experiments. Table 1 shows reaction conditions and the results obtained for three similar experiments. As can be seen in Table 1, similar productivity of the catalyst is obtained.

Effect of hydrogen concentration

To study the effect of hydrogen concentration on R_p, four runs with different H_2 concentrations were carried out at 70°C. The results are shown in Table 2.

From Table 2 it can be concluded that by increasing hydrogen concentration, initial polymerization rate (R_{pmax}) has increased. This is in agreement with the results presented by others [4,9,13].

The effect of hydrogen concentration on normalized polymerization profiles (R_p/R_{pmax}) is illustrated in Figure 6. Figure 6 shows the impact of hydrogen level with increasing H_2 concentration under the applied conditions. In the absence of hydrogen, the term "*a*", which was considered as activation intensity, is about twice at the zero hydrogen concentration. The term "*b*" which was defined as deactivation intensity showed an increase with hydrogen concentration, as can be seen in Table 2. The values of R_{pmax}/R_{pmax1} (R_{pmax1} is R_p at zero hydrogen) calculated in Table 2 show an activation factor of about 2 in the presence of hydrogen.

At high hydrogen concentrations, a plateau R_p/R_{pmax} was observed. This plateau effect has been confirmed by several authors like Guastalla and Rishina et al. [21, 22]. Our results were also in agreement with the results presented by Samson and Pater et al. [9, 15]. They proposed that the concentration of blocked active centers decreased at high hydrogen concentrations.

The ratio of *a/b* in equation 24 (representing activation to decay ratio) is also calculated in Table 2. The results showed an increase of about 1.5 times in the ratio of "*a/b*" when no hydrogen was added to the reactor. From Table 2 we can conclude the inverse result related to the rate of polymerization and the "*a/b*" ratio.

Our results indicated that the increase in productivity by hydrogen is mainly due to the increase in the initial polymerization rate, while hydrogen under the conditions used in this study has no negative or small effect on the rate of decay.

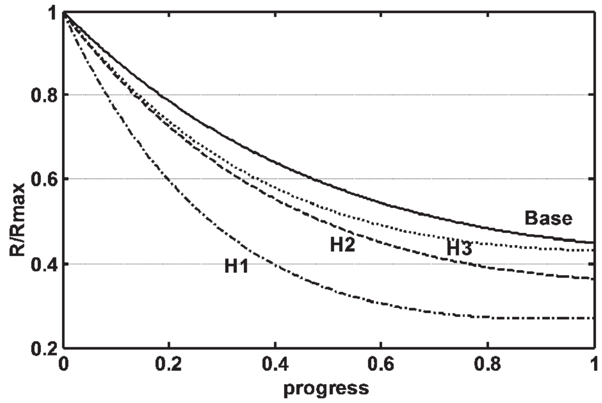

Figure 6. Rate profiles at different hydrogen concentrations at 70°C. $\frac{R}{R_{\max}} = 1+e^{-at}-e^{-bt} \quad , \quad a,b>0$

Effect of External Electron Donor concentration

Effect of External Electron Donor (ED) concentration on R_p was studied by conducting three experiments at 70°C and at different ED concentrations. The polymerization conditions for these experiments are summarized in Table 3. In Figure 7, the changes in the normalized polymerization profiles (R_p/R_{pmax}) with the changes in the ED concentration are plotted. It can be seen from Figure 6 that there was an optimum amount of ED in which maximum R_p/R_{pmax} was obtained. From Figure 7 and Table 3 it also can be concluded that at the optimum ED concentration, the term "*b*" (representing deactivation intensity) is at the minimum level, results in the R_p/R_{pmax} curve being in its optimum shape. The term "*a/b*" showed slight

Table 1. Polymerization at 70°C under similar conditions to prove reproducibility of experiments.

Run No.	Pressure (bar)	T (°C)	Hydrogen (mol)	Catalyst (mg)	Product (g)	Productivity (Kg_{pol}/g_{cat})
Test1	37	70	0.05	17	400	23.5
Test2	37	70	0.05	16.2	355	22
Test3	37	70	0.05	15.8	340	21.5

Table 2. Polymerization at 70°C at different H_2 concentrations and similar hydrogen concentration.

Run	Hydrogen (mol)	Catalyst (mg)	Product (g)	R_{pmax} (g_{PP} /mg_{cat}.h)	R_{pmax}/R_{pmax1}	(*a* , *b*)*	*a/b*	DH
H1	0	12.5	116.5	14.5	1	(3 , 0.25)	12	2916
H2	0.015	13.4	271	26.3	1.8	(1.95,0.25)	7.8	2559
Base	0.05	15.8	340	28.2	1.9	(1.75,0.27)	6.36	2170
H3	0.075	13	353	33.2	2.3	(2 , 0.35)	5.7	2419

**a* and *b* were calculated from equation 24.

Table 3. Polymerization at 70°C at different ED concentrations and similar hydrogen concentration.

Run	ED (ml)	Catalyst (mg)	TEAL/ED (mol/mol)	R_{pmax} (g_{PP} /mg_{cat}.h)	Product/Cat (g_{pol}/mg_{cat})	(*a* , *b*)	*a/b*
D1	0.09	11	10	31.82	22.91	(2.3 , 0.35)	6.57
Base	0.06	15.8	20	28.15	21.52	(1.75,0.275)	6.36
D3	0.04	9	30	36.05	41.66	(1.8 , 0.3)	6

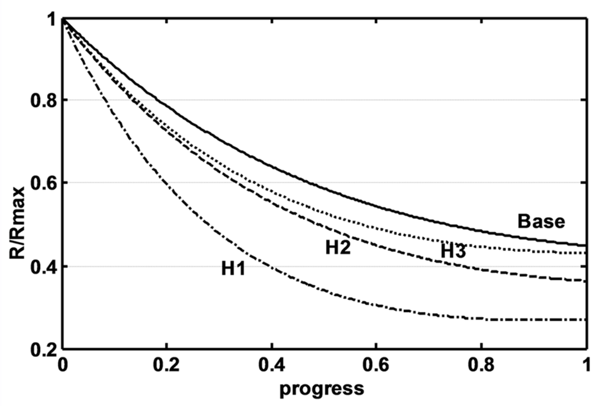

Figure 7. Rate profiles at different ED concentrations at 70°C.

changes with changes in ED concentration, meaning that activation and deactivation rate intensity changed proportionally at different concentrations of ED.

CONCLUSIONS

Bulk phase polymerization of propylene with a Mg/Cl_2-supported Z-N catalyst was kinetically investigated by means of heat flow calorimetry. To guarantee the operation of estimators, a calibration method was used. This preliminary calibration is based on the fact that "the heat generation is zero when reaction does not occur." The results showed that although estimations were valid in the steady conditions, dynamic regions could not be predicted. Our calibration method showed that heat exchange with the reactor cover plate was not constant over the reaction time. Therefore, the dynamic of cover plate temperature was considered in the calorimetric method. The polymerization rate profiles depending on hydrogen and external electron donor concentration were investigated. Normalized polymerization profiles (R_p/R_{pmax}) were plotted and expressed as an exponential function of time.

Effects of hydrogen and external donor concentration on initial polymerization rate (R_{pmax}) and polymerization rate were investigated. It was observed that hydrogen increases R_{pmax}. Effect of hydrogen concentration on R_p/R_{pmax} indicated that hydrogen leads to the increase in productivity by increasing the ratio of activation to deactivation. Under the conditions we used, hydrogen increased the activation constant, while having little or no negative effect on the rate of decay.

Also, changes in the concentration of ED (from optimum TEAL/Donor ratio) caused R_p/R_{pmax} and deactivation intensity to increase.

SYMBOLS AND ABBREVIATIONS

A_i	heat exchange area (m^2)
A_∞	heat exchange area with the environment (m^2)
b	constant, representing deactivation intensity
C_1	constant
C_2	constant
c_p	monomer heat capacity (JK^{-1})
c_w	heat capacity of water (JK^{-1})
ED	External Electron Donor
F_w	inlet water flow rate (m^3s^{-1})
H_r	enthalpy of the reaction ($Jmol^{-1}$)
H	load variable
m	monomer mass (g)
m_{cat}	mass of catalyst (g)
m_j	mass of water in the jacket (g)
mileage	weight of final product (g)
m_r	mass of the reactor contents plus agitator, etc. (g)
Q_{acc}	energy accumulated in the reactor during the reaction (J)
Q_b	the term represents the interaction of the system with the environment, a load variable (J)
Q_{jacket}	heat exchange through the reactor wall (J)
Q_{loss}	heat loss to the surroundings (J)
Q_r	total heat generated by the reaction, a load variable (J)

R_p	rate of reaction (mol $m^{-3}s^{-1}$)
R_{pi}	functions of individual monomer concentrations
t	time (s)
T	reactor temperature (ºC)
T_∞	environment temperature (ºC)
T_j	Jacket temperature (ºC)
T_{ji}	inlet jacket temperature (ºC)
T_{jo}	outlet jacket temperature (ºC)
T_m	reactor temperature reported by sensor (ºC)
$T_{j,m}$	jacket temperature reported by sensor (ºC)
T_M°	cover plate temperature (ºC)
τ_m	sensor response time constant
τ'_m	sensor response time constant
T_r	is nearly zero and was neglected
u_i	reactor wall heat exchange coefficient ($Js^{-1}m^{-2}K^{-1}$)
U	control variable (J $s^{-1}m^{-2}K^{-1}$)
U_∞	heat transfer coefficient with the environment ($Js^{-1}m^{-2}K^{-1}$)
ρ_w	density of water (Kgm^{-3})
λ	constant
Z-N	Ziegler-Natta catalyst

APPENDIX

$$A=\begin{bmatrix}\dfrac{1-a_{22}.\Delta t}{\beta} & \dfrac{a_{12}.\Delta t}{\beta}\\ \dfrac{a_{21}.\Delta t}{\beta} & \dfrac{1-a_{11}.\Delta t}{\beta}\end{bmatrix}\quad,\quad B=\begin{bmatrix}\dfrac{(1-a_{22}.\Delta t).\Delta t}{\beta} & \dfrac{a_{12}.(\Delta t)^2}{\beta}\\ \dfrac{a_{21}.(\Delta t)^2}{\beta} & \dfrac{(1-a_{11}.\Delta t).\Delta t}{\beta}\end{bmatrix}$$

$$C=\begin{bmatrix}\dfrac{\tau_m}{\tau_m+\Delta t} & 0\\ 0 & \dfrac{\tau'_m}{\tau'_m+\Delta t}\end{bmatrix}\quad,\quad D=\begin{bmatrix}\dfrac{\Delta t}{\tau_m+\Delta t} & 0\\ 0 & \dfrac{\Delta t}{\tau'_m+\Delta t}\end{bmatrix}$$

where

$$a_{11}=-\frac{u_i.A_i}{m.C_p}\quad,\quad a_{12}=\frac{u_i.A_i}{m.C_p}$$

$$a_{21}=\frac{u_i.A_i}{m_j.C_w}\quad,\quad a_{22}=-\frac{(1-\gamma)\,(u_i.A_i+u_\infty.A_\infty)+F_w.\rho_w.C_w}{m_j.C_w(1-\gamma)}$$

$$\beta=1-a_{11}.\Delta t-a_{22}.\Delta t+a_{11}.a_{22}.(\Delta t)^2-a_{12}.a_{21}.(\Delta t)^2$$

REFERENCES

1. Levenspiel O (1999) Chemical reaction engineering. Industrial & engineering chemistry research. Ind Eng Chem Res 38: 4140-4043
2. Choi KY, Ray WH (1985) Polymerization of olefins through heterogeneous catalysis. II. Kinetics of gas phase propylene polymerization with Ziegler–Natta catalysts. J Appl Polym Sci 30: 1065-1081
3. Soares JB, Hamielec AE (1996) Kinetics of propylene polymerization with a non-supported heterogeneous Ziegler-Natta catalyst-effect of hydrogen on rate of polymerization, stereoregularity, and molecular weight distribution. Polymer 37: 4607-4614
4. Lavoisier AL, De Laplace PS (1892) Abhandlungen über die Wärme 1780 and 1784. In: Ostwald's Klassiker der Exakten Wissenschafen 40: 28, ed. Rosenthal J Wilhelm Engelmann, Leipzig
5. Tisse VF, Sheibat-Othman N, McKenna TF (2010) A lab-scale reaction calorimeter for olefin polymerization. Canadian J Chem Eng 88: 783-792
6. Samson JJ, van Middelkoop B, Weickert G, Westerterp KR (1999) Gas-phase polymerization of propylene with a highly active Ziegler-Natta catalyst. AIChE J 45: 1548-1558
7. Karlsen LG, Villadsen J (1987) Isothermal reaction calorimeters-I. A literature review. Chem Eng Sci 42:1153-1164
8. Hansen LD, Hart RM (2004) The art of calorimetry. Thermochimica acta 17: 257-273
9. Samson JJ, Weickert G, Heerze AE, Westerterp KR (1998) Liquid-phase polymerization of propylene with a highly active catalyst. AIChE J 44:1424-1437
10. Meier GB, Weickert G, Van Swaaij WP (2001) Gas-phase polymerization of propylene: Reaction kinetics and molecular weight distribution. J Polym Sci Pol Chem 15: 500-513
11. Kettner J, Valaei S, Bartke M (2020) Reaction calorimetry for studying kinetics in bulk phase polymerization of propene. Macromol React Eng 26: 2000031
12. Ali MA, Betlem B, Roffel B, Weickert G (2007) Estimation of the polymerization rate of liquid propylene using adiabatic reaction calorimetry and reaction dilatometry. Macromol React Eng 8: 353-363
13. Samson JJ, Bosman PJ, Weickert G, Westerterp

KR (1999) Liquid-phase polymerization of propylene with a highly active Ziegler–Natta catalyst. Influence of hydrogen, cocatalyst, and electron donor on the reaction kinetics. J Polym Sci Pol Chem 15: 219-232

14. Shimizu F, Pater JT, Weickert G (2001) Three-site mechanism and molecular weight: Time dependency in liquid propylene batch polymerization using a $MgCl_2$-supported Ziegler-Natta catalyst. J Appl Polym Sci 81:1035-1047
15. Pater JT, Weickert G, Van Swaaij WP (2002) Polymerization of liquid propylene with a 4th generation Ziegler-Natta catalyst-influence of temperature, hydrogen and monomer concentration and prepolymerization method on polymerization kinetics. Chem Eng Sci 57: 3461-3477
16. Mckenna TF, Févotte G, Graillat C, Guillot J (1996) Joint use of calorimetry, densimetry and mathematical-modeling for multiple component polymerization. Chem Eng Res des 74: 340-348
17. Korber F, Hauschild K, Winter M, Fink G. (2001) Reaction calorimetric investigation of the propylene slurry phase polymerization with a silica-supported metallocene/MAO catalyst. Macromol Chem Phys 202: 3323-3328
18. Rouquerol J, Zielenkiewicz W (1986) Suggested practice for classification of calorimeters. Thermochimica Acta. 109: 121-37
19. Zogg A, Stoessel F, Fischer U, Hungerbühler K (2004) Isothermal reaction calorimetry as a tool for kinetic analysis. Thermochimica acta 419: 1-7
20. McKenna TF, Othman S, Fevotte G, Santos AM, Hammouri H (2000) An integrated approach to polymer reaction engineering: A review of calorimetry and state estimation. Polym React Eng 8: 1-38
21. Guastalla G, Giannini U (1983) The influence of hydrogen on the polymerization of propylene and ethylene with an $MgCl_2$ supported catalyst. Makromol Chem Rapid Commun 4: 519-527
22. Rishina LA, Vizen EI, Sosnovskaja LN, Dyachkovsky FS (1994) Study of the effect of hydrogen in propylene polymerization with the $MgCl_2$-supported Ziegler-Natta catalyst-part 1. Kinetics of polymerization. Eur Polym J 30: 1309-1313